Rational Polynomial Chaos Expansions for the Stochastic Macromodeling of Network Responses

Rational Polynomial Chaos Expansions for the Stochastic Macromodeling of Network Responses

Paolo Manfredi, *Senior Member, IEEE,* Stefano Grivet-Talocia, *Fellow, IEEE.*

***Abstract*—This paper introduces rational polynomial chaos expansions for the stochastic modeling of the frequency-domain responses of linear electrical networks. The proposed method models stochastic network responses as a ratio of polynomial chaos expansions, rather than the standard single polynomial expansion. This approach is motivated by the fact that network responses are best represented by rational functions of both frequency and parameters. In particular, it is proven that the rational stochastic model is exact for lumped networks. The model coefficients are computed via an iterative re-weighted linear least-square regression. Several application examples, concerning both lumped and a distributed systems, illustrate and validate the advocated methodology.**

***Index Terms*—Multiport systems, polynomial chaos, rational modeling, variability analysis, uncertainty quantification.**

I. Introduction

FOR more than a decade, polynomial chaos received a wide attention by the macromodeling community in electrical engineering because of its superior efficiency and accuracy over the Monte Carlo (MC) method in the variability analysis of the performance of electronic systems [1]–[3]. Polynomial chaos represents stochastic quantities as an expansion into orthogonal polynomials. Several implementations of polynomial chaos were proposed to study the stochastic behavior of electrical circuits. As opposed to Galerkin-based approaches [4]–[6], which convert a stochastic system of equations into an augmented set of coupled deterministic equations in the unknown polynomial chaos expansion (PCE) coefficients, "black-box" or sampling-based strategies collect suitable samples of the response and post-process them to to obtain the coefficients by means of interpolation [7]–[9] or regression [10]–[12]. Efficient tensor-based approaches were also proposed [13], [14], but their implementation is more cumbersome and, in some cases, limited to scalar outputs.

This paper focuses on modeling the frequency-domain responses of linear networks that are subject to parameter variability. Typically, a single PCE is used to model such stochastic responses, and the expansion coefficients are obtained by regression [10]. However, it is well-known that any frequency-domain response of a lumped electrical network is a rational function of both frequency and circuit element values, whose dependence of numerator and denominator is *multi-linear*. This representation is also well suited to approximate the response of systems that include distributed elements, albeit with higher-degree expansions. This follows from the general consideration that rational approximations are usually much more accurate than polynomial approximations, a fact that is routinely applied in moment-matching based model order reduction algorithms [15].

In this paper, a new model is put forward, where the stochastic network response is modeled as a ratio of PCEs, rather than as a single PCE, leading to the new paradigm of Rational Polynomial Chaos (RPC). For multivariate problems, it is shown that a tensor degree truncation strategy is preferable over the more popular total degree choice. A similar idea, based on Padé approximants, was proposed in fluid [16] and structural [17] dynamics, and used in [18] to model figures of merit of antennas. However, as will be discussed later on, our approach substantially differentiates from [16]–[18] in the motivation, truncation strategy, calculation of the expansion coefficients, and bias correction.

The remainder of the paper is organized as follows. Section II summarizes the basic notions of conventional polynomial chaos approaches. Section III shows that any response of a linear lumped circuit is described by a rational multi-linear function of the element values. Although this is well-known background material, some minimal statements are included to set notation and to provide a basis for further developments. Based on this result, Section IV introduces the proposed RPC, whereas Section V elaborates on the optimal truncation strategy of the PCEs. The differences w.r.t. to similar approaches available in the literature are discussed in Section VI. Applications and numerical results are provided in Section VII, while the performance is discussed in Section VIII. Finally, conclusions are drawn in Section IX.

II. Classical Polynomial Chaos Expansion

Consider an electrical system affected by d random parameters collected in vector $\boldsymbol{\xi} = [\xi_1, \ldots, \xi_d]$. Any frequency-domain network response depends on the parameters $\boldsymbol{\xi}$ and, according to state-of-the-art PC approaches, can be represented by a PCE [10]:

$$S(s;\boldsymbol{\xi}) \approx \hat{S}(s;\boldsymbol{\xi}) = \sum_{\ell=1}^{L} S_\ell(s)\varphi_\ell(\boldsymbol{\xi}), \tag{1}$$

where s is the Laplace variable, S denotes an arbitrary network response (e.g, an S- or Y-parameter), $\hat{S}$ is the corresponding PCE approximation, $\{\varphi_\ell\}_{\ell=1}^{L}$ is a set of multivariate orthogonal polynomials according to the inner product

$$\langle f, g\rangle = \int_{\mathbb{R}^d} f(\boldsymbol{\xi})g(\boldsymbol{\xi})w(\boldsymbol{\xi})d\boldsymbol{\xi}, \tag{2}$$

where $w(\boldsymbol{\xi})$ is the joint probability distribution of $\boldsymbol{\xi}$, and S_ℓ are the pertinent expansion coefficients to be determined.

P. Manfredi and S. Grivet-Talocia are with the Department of Electronics and Telecommunications, Politecnico di Torino, Turin 10129, Italy (e-mail: paolo.manfredi@polito.it; stefano.grivet@polito.it).

If the random parameters are mutually independent, $w(\boldsymbol{\xi}) = \prod_{i=1}^{d} w(\xi_i)$, where $w(\xi_i)$ is the probability distribution of the single random parameter ξ_i. In this common case, the multivariate polynomials φ_ℓ are constructed as the product of the univariate polynomials ϕ_{ℓ_i} that are orthogonal based on the one-dimensional inner product [19]

$$\langle f, g \rangle_i = \int_{-\infty}^{+\infty} f(\xi_i) g(\xi_i) w(\xi_i) d\xi_i, \qquad i = 1, \ldots, d. \quad (3)$$

This choice provides the fastest convergence rate, when L is increased, of the weighed error norm $\|S(s;\boldsymbol{\xi}) - \hat{S}(s;\boldsymbol{\xi})\|_w$, defined as

$$\|f\|_w = \sqrt{\langle f, f \rangle} \quad (4)$$

based on the inner product (2).

It is possible to map the scalar index ℓ into a multi-index $\boldsymbol{\ell} = [\ell_1, \ldots, \ell_d]$, such that

$$\varphi_{\ell \leftrightarrow \boldsymbol{\ell}} = \prod_{i=1}^{d} \phi_{\ell_i}(\xi_i). \quad (5)$$

It should be noted that each ϕ_{ℓ_i} is a polynomial of degree ℓ_i. Typically, only the polynomials up to a given "total degree" p are retained in the expansion (1), meaning that

$$\|\boldsymbol{\ell}\|_1 = \sum_{i=1}^{d} \ell_i \leq p \quad (6)$$

and leading to a total number of terms in the expansion equal to $L = (p+d)!/(p!d!)$. For dependent/correlated random parameters, numerical approaches exist for the calculation of suitable multivariate orthogonal polynomials [20], and the proposed RPC technique applies with minimal modifications.

The coefficients of (1) are usually calculated by least-square regression. The response $S(s, \boldsymbol{\xi})$ is calculated for a set of $K \gg L$ samples $\{\boldsymbol{\xi}^{(k)}\}_{k=1}^{K}$ of the random parameters for the regression problem to be overdetermined, and the results are fitted to the model (1) in a least-square sense. As a rule of thumb, it is often suggested to take $K = 2L$ [10]. However, more samples might be needed when the variability is high and/or the system has significant delay, as illustrated later on. Other approaches identify a special selection of $K = L$ random variable samples, resulting in an interpolation of the corresponding responses [8], [9].

III. General Form of the Transfer Function of Linear Lumped Circuits

In this section, we reveal in explicit form the functional dependence on the individual stochastic parameters of any transfer function that can be defined on a lumped linear time-invariant (LTI) circuit. This will be the main guideline to introduce and justify the proposed RPC form, which is then extended to any general LTI system (either lumped or distributed) with uncertain parameters.

Let us consider a P-port lumped LTI circuit block with the objective of characterizing its $P \times P$ impedance matrix $\boldsymbol{Z}(s)$ in the Laplace domain, and let us collect in vector $\boldsymbol{\theta}$ its circuit parameters that are subject to variations; these include resistances, capacitances, self and mutual inductances, and possibly linear controlled source gains. We define a nominal parameter configuration $\boldsymbol{\theta} = \bar{\boldsymbol{\theta}}$ for which the circuit is uniquely solvable. For instance, this nominal configuration can be considered as the set of expected values of the circuit element values, assumed to be stochastic variables. We introduce the variable transformation $\boldsymbol{\theta} = \bar{\boldsymbol{\theta}} + \boldsymbol{\xi}$, where each element of vector $\boldsymbol{\xi}$ is a zero-mean stochastic variable.

The Laplace-domain impedance matrix of the considered P-port circuit block can be cast as

$$\boldsymbol{Z}(s;\boldsymbol{\xi}) = \frac{\mathsf{N}(s;\boldsymbol{\xi})}{\mathsf{D}(s;\boldsymbol{\xi})}. \quad (7)$$

A symbolic analysis [21] (see also [22] and references therein) can be performed in order to reveal the explicit dependence of numerator and denominator in (7) on complex frequency s and stochastic variables $\boldsymbol{\xi}$. It is easy to show that the scalar denominator can be written as

$$\mathsf{D}(s;\boldsymbol{\xi}) = \sum_i \mathsf{d}_i(s) \prod_{\nu=1}^{d} \xi_\nu^{\alpha_{i\nu}}, \quad \alpha_{i\nu} \in \{0,1\} \quad \forall i\nu \quad (8)$$

where, due to the lumped nature of the system under consideration, the coefficients $\mathsf{d}_i(s)$ are polynomials in s of degree up to the dynamic order N of the circuit. The same structural dependence on frequency s and parameters ξ_ν applies to the individual elements of the $P \times P$ numerator matrix $\mathbf{N}(s;\boldsymbol{\xi})$ in (7). Therefore, any element (i,j) of the impedance matrix $\boldsymbol{Z}(s;\boldsymbol{\xi})$ has the following structure

$$Z_{ij}(s;\boldsymbol{\xi}) = \frac{\sum_{k=0}^{N_{ij}} a_{k;ij}(\boldsymbol{\xi}) s^k}{\sum_{k=0}^{N} b_k(\boldsymbol{\xi}) s^k}, \quad (9)$$

where all numerator and denominator coefficients $a_{k;ij}(\boldsymbol{\xi})$ and $b_k(\boldsymbol{\xi})$ have a *multi-linear* dependence on the stochastic parameters, i.e., they are multivariate polynomials in which each parameter ξ_ν appears with up to order one in any of these coefficients. Stated differently, any impedance element is a rational function of any stochastic parameter ξ_ν with both numerator and denominator degrees that cannot exceed one. We remark that the same structural form (9) applies to any alternative definition of port inputs and outputs, including any immittance (admittance and hybrid) as well as scattering representations.

IV. Rational Polynomial Chaos Expansion

As shown in the previous section, any frequency-domain response of a linear electrical network is a rational function w.r.t. both frequency and parameters. Therefore, it is argued that a rational approximation in the form

$$S(s,\boldsymbol{\xi}) \approx \hat{S}(s;\boldsymbol{\xi}) = \frac{\mathsf{N}(s;\boldsymbol{\xi})}{\mathsf{D}(s;\boldsymbol{\xi})} = \frac{\sum_{\ell=1}^{L} N_\ell(s) \varphi_\ell(\boldsymbol{\xi})}{1 + \sum_{\ell=2}^{L} D_\ell(s) \varphi_\ell(\boldsymbol{\xi})} \quad (10)$$

provides a better model[1] in place of (1). In fact, the representation (10) coincides with (9) for lumped circuits parameterized by their element values, provided that $\varphi_\ell(\boldsymbol{\xi})$ are multi-linear basis functions. In the following, we will extend its scope by showing applicability to more general structures (including distributed circuits) by adopting higher-degree polynomials, and demonstrating significantly better performance than standard PCE.

[1]The first expansion term in the denominator has been set to 1 to remove indeterminacy. Otherwise, numerator and denominator could only be determined up to an arbitrary scaling factor.

A. Iterative Re-Weighted Linear Least-Square Regression

The model (10) is nonlinear in the coefficients D_ℓ, hence linear regression cannot be directly used for their calculation. Nevertheless, it is possible to rearrange (10) as

$$\sum_{\ell=1}^{L} N_\ell(s)\varphi_\ell(\boldsymbol{\xi}) - S(s;\boldsymbol{\xi})\sum_{\ell=2}^{L} D_\ell(s)\varphi_\ell(\boldsymbol{\xi}) \approx S(s;\boldsymbol{\xi}), \quad (11)$$

which is now linear in the coefficients N_ℓ and D_ℓ. Such coefficients can be estimated by solving the regression problem

$$\begin{pmatrix}\boldsymbol{N}^*\\ \boldsymbol{D}^*\end{pmatrix} = \arg\min \left\| \begin{pmatrix}\boldsymbol{\Psi} & -\boldsymbol{\Psi}'\end{pmatrix} \begin{pmatrix}\boldsymbol{N}\\ \boldsymbol{D}\end{pmatrix} - \boldsymbol{w} \right\| \quad (12)$$

over K samples, where

$$\begin{aligned}\boldsymbol{N} &= \left(N_1,\dots,N_L\right)^{\mathsf{T}},\\ \boldsymbol{D} &= \left(D_2,\dots,D_L\right)^{\mathsf{T}},\\ \boldsymbol{w} &= \left(S(s,\boldsymbol{\xi}^{(1)}),\dots,S(s,\boldsymbol{\xi}^{(K)})\right)^{\mathsf{T}},\end{aligned}$$

whereas $\boldsymbol{\Psi} \in \mathbb{R}^{K\times L}$ has entries

$$\Psi_{k,\ell} = \varphi_\ell(\boldsymbol{\xi}^{(k)}),$$

for $k = 1,\dots,K$ and $\ell = 1,\dots,L$, while $\boldsymbol{\Psi}' \in \mathbb{R}^{K\times(L-1)}$ has entries

$$\Psi'_{k,\ell} = S(s,\boldsymbol{\xi}^{(k)})\varphi_\ell(\boldsymbol{\xi}^{(k)}),$$

for $k = 1,\dots,K$ and $\ell = 2,\dots,L$.

The regression samples $\{\boldsymbol{\xi}^{(k)}\}_{k=1}^{K}$ are drawn according to the distribution of $\boldsymbol{\xi}$ using a Latin hypercube sampling (LHS) strategy. This makes sure that the coefficients that minimize the residual norm in (12) are close to the "exact" coefficients minimizing norm (4) of the PCE error. This is illustrated by means of an analytic example in the next section. However, the result of the linear regression problem (12) is biased w.r.t. the nonlinear problem (10), since the former minimizes a different residual norm, i.e., $\|\mathsf{D}(s,\boldsymbol{\xi})R(s,\boldsymbol{\xi})\|$ instead of $\|R(s,\boldsymbol{\xi})\|$, with $R(s,\boldsymbol{\xi}) = S(s,\boldsymbol{\xi}) - \mathsf{N}(s,\boldsymbol{\xi})/\mathsf{D}(s,\boldsymbol{\xi})$. Therefore, an iterative solution is put forward, where the common denominator is not eliminated from (11), leading to the modified regression problem

$$\begin{pmatrix}\boldsymbol{N}^\mu\\ \boldsymbol{D}^\mu\end{pmatrix} = \arg\min \left\| \begin{pmatrix}\boldsymbol{\Lambda}^\mu\boldsymbol{\Psi} & -\boldsymbol{\Lambda}^\mu\boldsymbol{\Psi}'\end{pmatrix} \begin{pmatrix}\boldsymbol{N}\\ \boldsymbol{D}\end{pmatrix} - \boldsymbol{\Lambda}^\mu\boldsymbol{w} \right\|, \quad (13)$$

where μ denotes the iteration index, and $\boldsymbol{\Lambda}^\mu \in \mathbb{R}^{K\times K}$ is a diagonal matrix with entries $\lambda^\mu_{k,k} = [\mathsf{D}^{\mu-1}(s,\boldsymbol{\xi}^{(k)})]^{-1}$. This matrix is fully known from the previous iteration step, and it can be initialized as the identity matrix (corresponding to a unitary denominator). This iteratively re-weighted regression problem is readily recognized as a stochastic reformulation of the well-known Sanathanan-Koerner (S-K) iteration [23], which is widely used in deterministic (parameterized) macro-modeling schemes [24]. It can be shown that the bias is reduced as the iterations increase, and is removed at convergence [23], [25]. It should be noted that such iterations do not require additional evaluations of the transfer function. In this paper, the above iterative regression problem is solved at each frequency point separately.

B. Distribution of the Regression Samples

This section shows the importance of drawing the regression samples in (12) according to the distribution of the random parameters $\boldsymbol{\xi}$. We consider the univariate analytical function

$$f(\xi) = \cosh(1+\xi),$$

with ξ being a standard normal random variable with zero mean and unitary variance. The example is deliberately designed to exhibit large variability. Figure 1 shows with a blue line the actual value of $f(\xi)$ in the range $[-3,3]$, i.e., the interval wherein there is a 99.7% probability to find values of ξ. The second column of Table I provides the mean and standard deviation of $f(\xi)$ estimated with MC sampling.

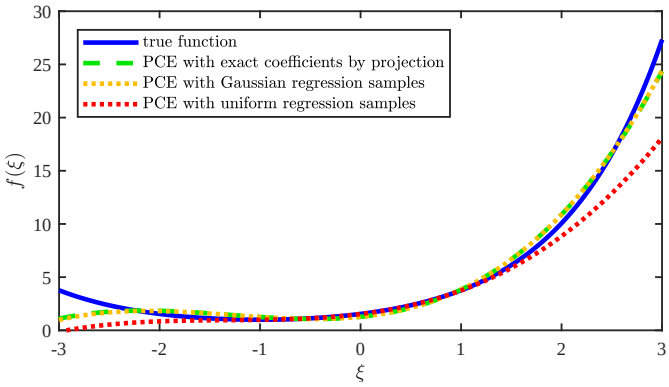

Fig. 1. Approximation of the stochastic function $f(\xi) = \cosh(1+\xi)$. Solid blue line: true function; dashed green line: third-order Hermite PCE with exact coefficients computed by numerical projection; dotted orange and red lines: third-order Hermite PCEs with coefficients computed by regression with normally- and uniformly-distributed samples, respectively.

For the modeling via polynomial chaos, we use a third-order single PCE (i.e., with $\mathsf{D} = 1$) with orthonormal Hermite basis functions:

$$\begin{aligned}\varphi_1(\xi) &= 1\\ \varphi_2(\xi) &= \xi\\ \varphi_3(\xi) &= (\xi^2-1)/\sqrt{2}\\ \varphi_4(\xi) &= (\xi^3-3\xi)/\sqrt{6}.\end{aligned}$$

The "exact" PCE, computed by numerically projecting the function $f(\xi)$ onto the above basis polynomials with the inner product (3), has the coefficients $N_{1,2,3,4}$ reported in the third column of Table I. The error norm and statistical estimates are also provided, and the corresponding approximation is shown in Fig. 1 with a dashed green line.

Next, the coefficients of the same PCE are estimated by means of linear regressions with either normally- or uniformly-distributed samples. The respective results are provided in the fourth and fifth columns of Table I, and shown by the dotted orange and red curves in Fig. 1. It is observed that the PCE computed with Gaussian-distributed regression samples matches the exact PCE, and the error norm is very close to the actual minimum. Conversely, the PCE computed with uniformly-distributed regression samples exhibits a large error, especially for $|\xi| > 2$, and this results in an inaccurate estimation of the statistics. In general, exact model coefficients can

be computed regardless of the samples distribution only when the form of the function and of the model entirely match. We emphasize that this example does *not* support the conclusion that linear regression does not work in deterministic approximation problems for which uniform samples are chosen. It rather shows that a significant bias in statistical estimates is to be expected when regression samples are drawn based on incorrect distributions. When the approximation problem at hand is deterministic, different choices of the samples used for regression will inevitably induce differences in the approximation error, which will be reduced in the regions that are more densely sampled with respect to coarsely sampled regions.

TABLE I
STATISTICS AND PCE APPROXIMATIONS FOR $f(\xi) = \cosh(1+\xi)$.

	MC	exact PCE	Gaussian-distributed regression samples	uniformly-distributed regression samples
N_1	–	2.5441	2.5443	2.3647
N_2	–	1.9376	1.9430	1.7940
N_3	–	1.7990	1.7934	1.1699
N_4	–	0.7910	0.8012	0.5074
error	–	0.3109	0.3110	0.8399
mean	2.5474	2.5441	2.5443	2.3647
std	2.8327	2.7597	2.7629	2.2010

V. TRUNCATION STRATEGY

The derivations of Section III also allow concluding that the conventional total degree truncation expressed by (6) is not convenient for RPC expansions. For a lumped network, this can be understood by recalling that random parameters never appear with degree higher than one, as both the numerator and the denominator of any rational circuit response are multi-linear functions of the network parameters. However, setting $p = 1$ in (6), would cause the expansion to include only terms that are linear in a single variable, but not in more than one variable simultaneously. To remedy this issue, a "tensor degree" truncation, including all multivariate polynomials with multi-indices such that

$$\|\boldsymbol{\ell}\|_\infty = \max_i\{\ell_i\} \leq p \tag{14}$$

is adopted. Indeed, with this strategy and with $p = 1$, the basis functions $\varphi(\boldsymbol{\xi})$ turn out to be multi-linear and hence the PCE includes all the mixed terms that are expected to appear at the numerator and denominator, thus resulting to be *exact* for lumped circuits.

For structures that include distributed elements instead, the representation is no longer exact. Nonetheless, a tensor-product truncation is still a reasonable choice, but a higher order p may be required. With this truncation, the total number of terms in the expansion (14) becomes $2L-1 = 2(p+1)^d-1$. A detailed investigation on the optimal truncation strategies in RPC expansions is deferred to a future report.

VI. COMPARISON WITH AVAILABLE PADÉ FORMULATIONS

At this stage, it is important to remark the differences with the available Padé-approximant formulations [16]–[18].

- First of all, the proposed approach is motivated by the precise structure of the transfer function of any linear electrical system, outlined in Section III, and not just by the fact that the modeled function is possibly discontinuous, as is the case for example in [16];
- the proposed implementation uses a linear-regression approach to calculate the model coefficients, and this formulation readily scales to an arbitrary parameter dimension d. Conversely, the techniques in [16]–[18] rely on a multidimensional quadrature rule, whose generalization to high dimensions is not straightforward [16];
- the proposed implementation uses a straightforward S-K iteration to *systematically* remove the bias introduced by the elimination of the denominator in (12), instead of the denominator-dependent filtering procedure proposed in [16]. The bias issue is not addressed in [17] and [18].

VII. NUMERICAL RESULTS

This section validates the proposed RPC modeling based on several electrical networks, both lumped and distributed. For each test case, reference results are generated based on 10000 MC runs for as many samples of the random parameters $\boldsymbol{\xi}$. This number allows obtaining a sufficiently accurate reference for all considered test cases. Plain random sampling is used (LHS was also tested but turned out not to provide significant advantages). For a fair comparison, both the conventional PCE and the RPC model are evaluated for the very same samples, and the statistics of the obtained responses are compared against the reference MC estimates. This avoids introducing further errors due to the finite precision of the MC estimate itself.

A. Chebyshev Low-Pass Filter

The first application example considers a seventh-order Chebyshev low-pass filter. The filter has the schematic illustrated in Fig. 2 and is designed to exhibit a cut-off frequency of 2 GHz and a passband ripple of 0.5 dB. For the synthesis of Fig. 2, we considered components available on the market (cfr. Murata GRM capacitor series and LQW15A inductor series) and the indicated tolerances are taken from the actual datasheets provided by the vendor. The tolerance is considered as the standard deviation of a Gaussian random variable. This example has therefore $d = 7$ independent Gaussian random variables, which describe the uncertainty of the component values.

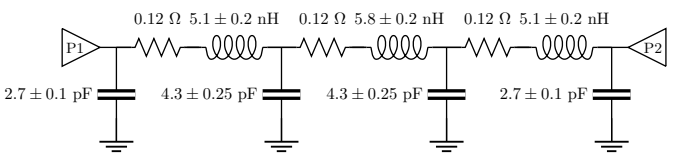

Fig. 2. Schematic of the seventh-order Chebyshev low-pass filter.

Fig. 3 shows the resulting variability of the magnitude of the Y-parameters. The mean and standard deviation obtained from the MC samples are compared with the results obtained from the conventional PCE with total degree $p = 4$ and the proposed RPC with tensor degree $p = 1$. The number of samples for the linear regression is taken as twice the number of the expansion coefficients to be computed, i.e., $K = 2L = 660$ (with $L = 11!/(4! \cdot 7!) = 330$) for the fourth-order single PCE, and $K = 2(2L - 1) = 510$ (with $L = 2^7 = 128$) for the RPC model. It is observed that the MC and RPC results are coincident, whereas the standard deviation of the PCE result exhibits a large error, especially around resonances and notwithstanding the high order. This is expected because this circuit is lumped, and the RPC model is therefore exact as opposed to the conventional PCE.

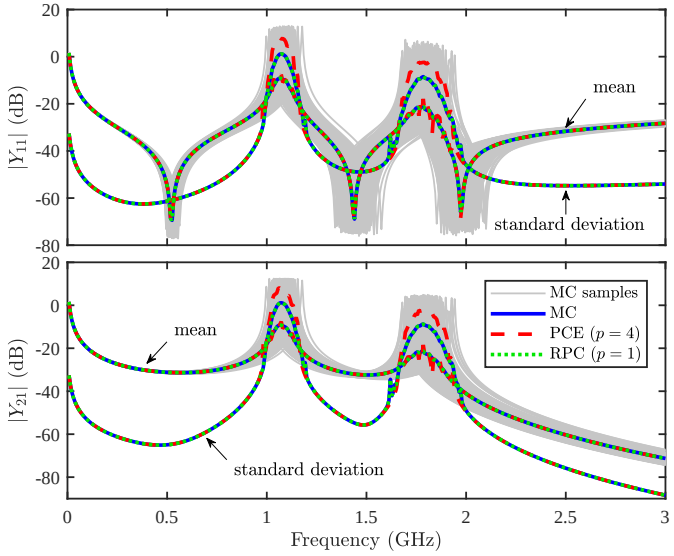

Fig. 3. Magnitude of Y_{11} (top panel) and Y_{21} (bottom panel) for the Chebyshev filter of Fig. 2. Gray lines: subset of MC samples; blue, red, and green lines: mean and standard deviation obtained from the MC samples, the conventional PCE, and the proposed RPC, respectively.

In principle, it is possible to improve the accuracy of the single PCE model by increasing the expansion order. Figure 4 shows with a dashed red line the standard deviation of Y_{11} and Y_{21} obtained with a sixth-order single PCE ($p = 6$) with coefficients estimated using $K = 2L = 3432$ regression samples. It is observed that such a PCE actually exhibits a larger error (detailed information in this regard is provided in Section VIII). This is explained by the fact that the estimation of a larger number of model coefficients in turn requires an even larger number of regression samples to be accurate. Indeed, by increasing the number of regression samples to as many as eight times the number of model coefficients (i.e., $K = 8L = 13728$) yields the dotted red curve in Fig. 4, showing an accuracy improvement compared to the fourth-order expansion of Fig. 3. This example shows that it is non-trivial to improve the accuracy of single PCEs, since increasing the expansion order may lead to an exorbitant requirement in terms of regression samples (note that the dotted curve in Fig. 4 is obtained using a larger number of samples than the MC reference!).

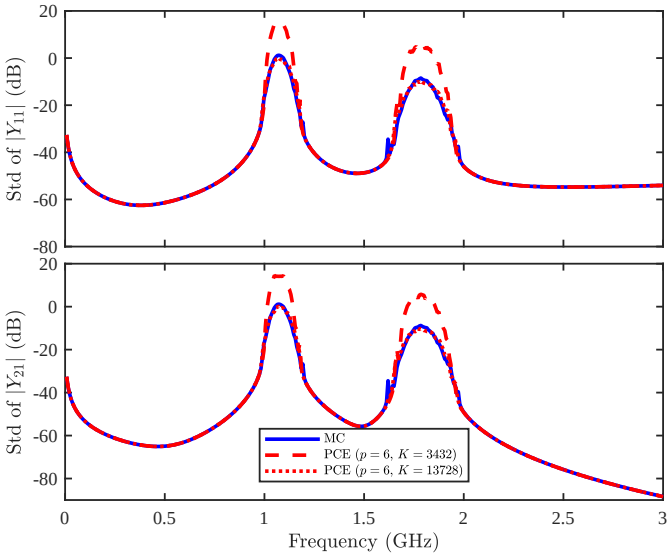

Fig. 4. Standard deviation of Y_{11} (top panel) and Y_{21} (bottom panel) obtained from a sixth-order single PCE with coefficients computed using $K = 3432$ (dashed red lines) and $K = 13728$ (dotted red lines) regression samples. The blue lines are the reference MC curves as in Fig. 3.

B. Network with Coupled Microstrip Lines

The second example deals with the distributed network of Fig. 5. The circuit includes delay elements, i.e., three coupled microstrip lines having the cross-section depicted in the top-left corner of Fig. 5. Two different scenarios are considered.

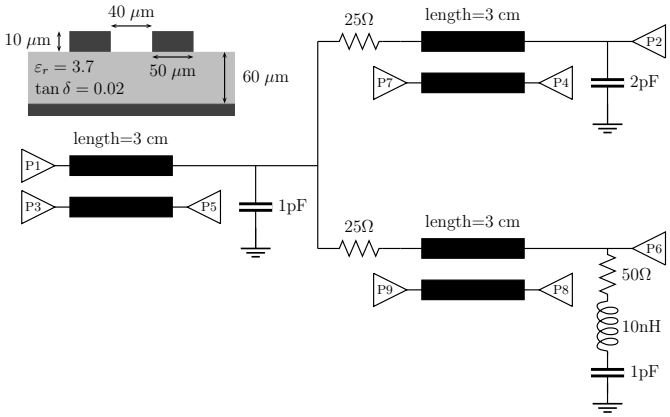

Fig. 5. Schematic of the distributed network with coupled transmission lines.

First, the uncertainty is assumed to be on lumped elements, namely the capacitors and the inductor, leading to $d = 4$ random parameters. These are assumed to be independent and Gaussian distributed, with a relative standard deviation of 20% w.r.t. to the (nominal) values indicated in Fig. 5. Being the uncertainty on lumped parameters only, the RPC model is still expected to be exact for a first-order tensor degree expansion, even though the system is distributed.

Figure 6, reporting the variability of the magnitudes of S-parameters S_{11}, S_{21}, S_{31}, and S_{41}, confirms this statement.

The plots show that a single PCE of order $p = 3$ is in this case very accurate as well. Nevertheless, a more rigorous analysis shows that, over the considered frequency sweep, the largest root-mean square (RMS) error of the conventional PCE on the standard deviation is 1.909×10^{-4}, whereas the maximum absolute error is 9.803×10^{-4}. The corresponding accuracy of the RPC model, for the same two error measures, is 4.686×10^{-9} and 1.606×10^{-8}. For the regression, $K = 2L = 70$ samples are used for the classical PCE, and $K = 2(2L-1) = 62$ samples for the RPC model.

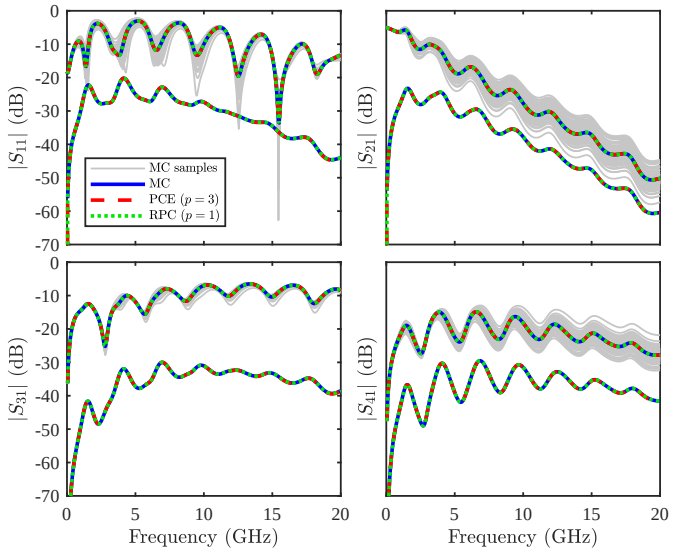

Fig. 6. Variability of some of the S-parameters for the distributed network of Fig. 5 with uncertainty in lumped components (inductors and capacitors). Curve identification is as in Fig. 3. Upper and lower colored curves are mean and standard deviation, respectively.

In the second scenario, the uncertainty is considered to be on the gap between the microstrip traces (Gaussian with a 10% relative standard deviation) and on the line length (Gaussian with a 5% relative standard deviation), leading to $d = 2$ random parameters. Being the uncertainty in the distributed elements, the RPC is no longer expected to be exact.

Figure 7 shows the resulting variability on the same S-parameters as considered in the first scenario. The uncertainty on the microstrip parameters causes a much larger variability on the network response, especially on S_{11}. In particular, the effect of the length uncertainty, leading to a shift in the resonances, is evident. For this scenario, a third-order expansion is used for the RPC, leading to a very high accuracy. On the other hand, a sixth-order single PCE still exhibits large errors, especially at higher frequencies.

The far superior accuracy of the RPC model can be further appreciated in Fig. 8, which shows the probability density function (PDF) of $|S_{11}|$ at 15 GHz, i.e., a frequency of very high variability according to Fig. 7. It is clear that the RPC curve is in much better agreement with the reference MC distribution.

The regression samples used for computing the model coefficients were $K = 8L = 224$ for the single PCE, and $K = 8(2L-1) = 248$ for the RPC model. In this case, we

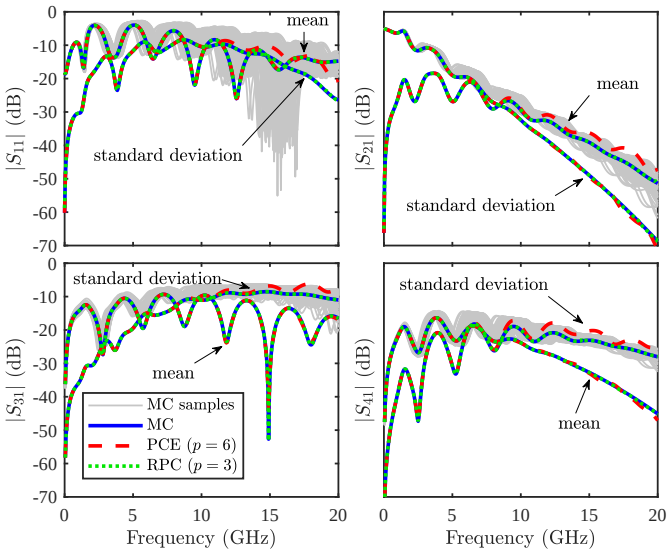

Fig. 7. Variability of some of the S-parameters for the distributed network of Fig. 5 with uncertainty in the distributed components (microstrip trace gap and length).

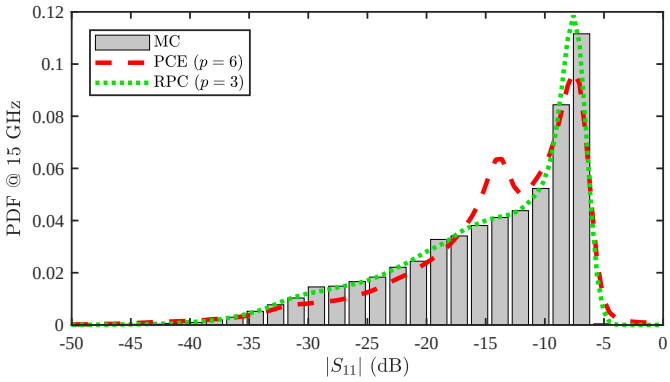

Fig. 8. PDF of $|S_{11}|$ at 15 GHz. Gray bars: MC result; dashed red line: single PCE; dotted green line: RPC model.

used as many samples as eight times the number of unknowns because the larger variability turns out to strongly affect the accuracy of the calculation.

As in the previous case, we try to improve the accuracy of the standard PCE by increasing the expansion order to $p = 8$. Figure 9 shows the standard deviation of the S-parameters obtained by calculating the expansion coefficients using $K = 8L = 360$ and $K = 32L = 1440$ regression samples (dashed and dotted red lines, respectively). This experiment confirms that increasing the expansion order also requires increasing the ratio between the number of regression samples and model coefficients to really achieve an improvement in the accuracy.

To further investigate the impact of the number of regression samples, Fig. 10 shows the evolution of the RMS and maximum error for different expansion orders and regression sample sizes. Specifically, we took a number of regression samples equal to 2, 4, and 8 times the number of RPC model coefficients for a given expansion order. Next, the coefficients of single PCEs of different orders are computed using the

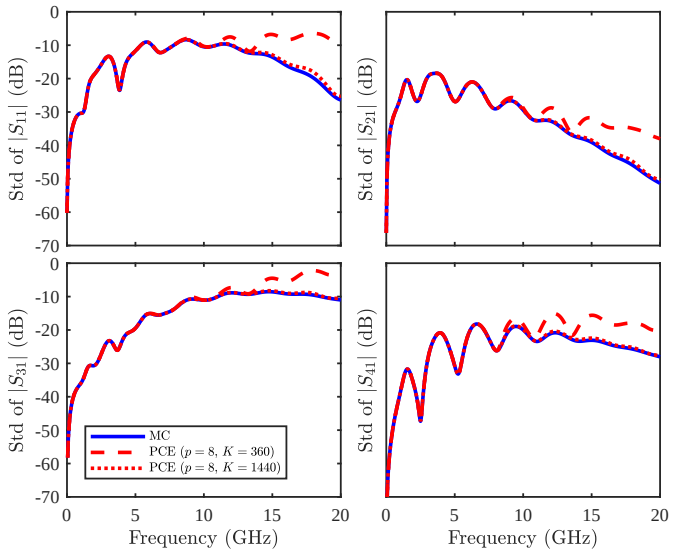

Fig. 9. Standard deviation of S_{11}, S_{21}, S_{31}, and S_{41}. Results obtained with a eigth-order single PCE computed using $K = 360$ and $K = 1440$ regression samples (dashed and dotted red lines, respectively) are compared against the reference MC result (blue line).

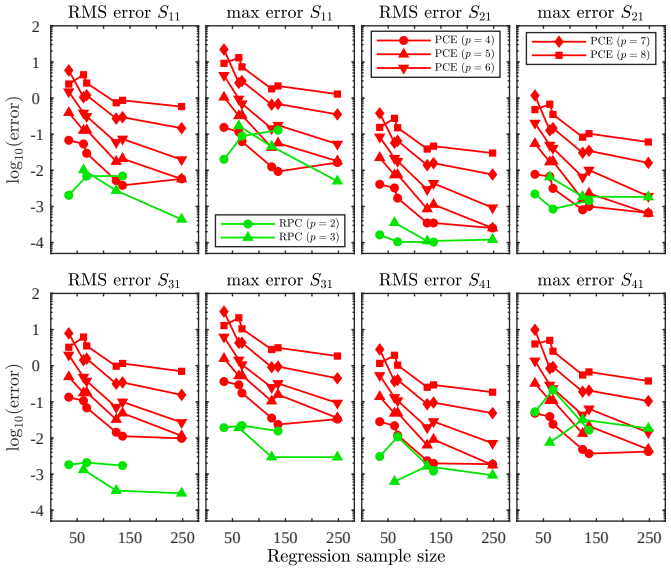

Fig. 10. Behavior of the RMS and maximum error for different expansion orders as a function of the regression sample size (network of Fig. 5).

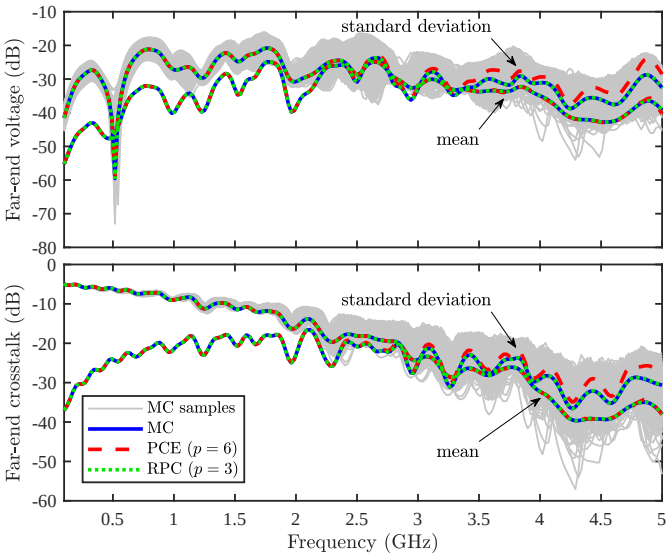

Fig. 11. Magnitude of the far-end voltage (top panel) and far-end crosstalk (bottom panel) transfer function for the high-speed link in [12]. Gray lines: subset of MC samples; blue, red, and green lines: mean and standard deviation obtained from the MC samples, the conventional PCE, and the proposed RPC, respectively.

same set of regression samples. It is observed that the RPC model is generally more accurate than the single PCE for a given sample size. For some S-parameters, the best achieved maximum error is similar for the single PCE and the RPC model, but the latter has always a much lower RMS error, meaning that it is globally more accurate over frequency.

It is also observed that the error does not always monotonically decrease with the regression sample size, although the *asymptotic* trend is decreasing. This is an inherent feature of stochastic techniques that use random sampling (including MC), as nothing prevents a local accuracy reduction when using a new set of random samples. Moreover, it is noticed that for single PCEs a lower order often provides better accuracy. As already mentioned, this is readily explained by the fact that the coefficients of a higher-order expansion, being larger in number, are estimated with lower accuracy with a given set of regression samples.

C. High-Speed Electronic Link

The third application example deals with the high-speed electronic link that was investigated in [12] (see Fig. 3 therein). The link represents a node-to-node bus consisting of interconnections, transmission lines, and vias. We refer to [12] for a detailed description of the network. The uncertain parameters are assumed to be the gap of the coupled microstrip lines (Gaussian with a relative standard deviation of 20%), and the length of each of the two sections (Gaussian with an absolute standard deviation of 5 mm), leading to a total of $d = 3$ parameters.

Figure 11 shows the variability of the far-end voltage (top panel) and far-end crosstalk (bottom panel) transfer functions. Expansion orders of $p = 6$ and $p = 3$ are used for the single PCE and the RPC model, respectively. The superior accuracy of the proposed RPC model is again confirmed by the PDFs shown in Fig. 12. These PDFs are computed at the frequency of 4.29 GHz, for which both the far-end voltage and crosstalk exhibit very large variability (cfr. Fig. 11). Indeed, the RPC results are in far better agreement with the reference MC distributions.

The number of regression samples used to calculate the model coefficients were $K = 8L = 672$ for the single PCE and $K = 8(2L - 1) = 1016$ for the RPC. Figure 13 shows the behavior of the RMS and maximum error as a function of the regression sample size. As in the previous test case, for a given sample size a third-order RPC model tends to be more accurate than a single PCE of similar or even higher order.

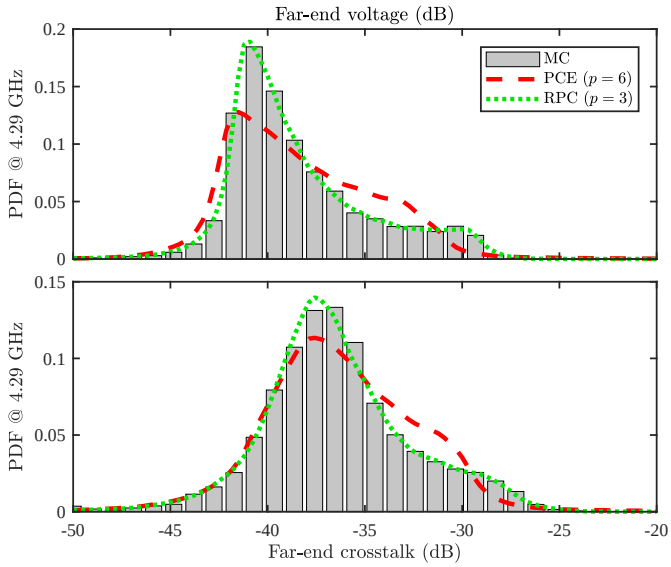

Fig. 12. PDFs of the far-end voltage and crosstalk magnitudes at 4.29 GHz. Gray bars: MC result; dashed red line: single PCE; dotted green line: RPC model.

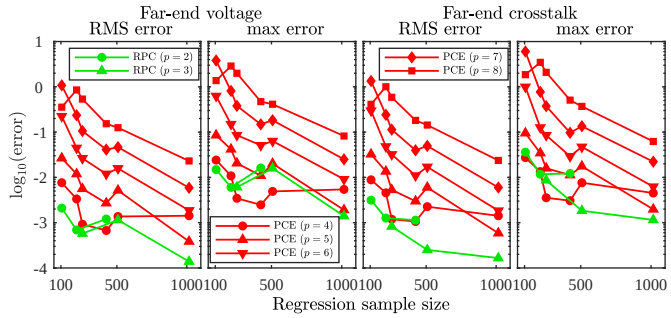

Fig. 13. Behavior of the RMS and maximum error for different expansion orders as a function of the regression sample size (high-speed link in [12]).

VIII. Performance Assessment

From the computational viewpoint, the main drawback of the proposed RPC compared to the standard PCE is that the regression matrix $\mathbf{\Psi}'$ in (12) is frequency dependent. Therefore, the regression problem needs to be solved frequency by frequency. Moreover, the solution includes additional iterations to remove bias in the estimation of the model coefficients, as explained in Section IV. Because of this, compared to the conventional PCE, the performance of the RPC does not scale much favorably with the number of frequency points and PCE size L.

Table II collects all relevant information regarding the considered test cases, including model accuracy and computational time. The accuracy is defined as the largest RMS error and absolute error on the standard deviation over all the responses considered in the plots of Section VII. The processing time comprises:

1) The evaluation of the samples for the regression. This is the main contribution to the time of standard PCE.
2) The calculation of the model coefficients. This has negligible impact on the conventional PCE time, but it is the bottleneck for the RPC due to the frequency-by-frequency solution of the regression problem.
3) The estimation of the mean and standard deviation, which is negligible for both the standard PCE and RPC models.

All simulations were performed on a Dell Precision 5820 workstation with an Intel(R) Core(TM) i9-7900X, CPU running at 3.30 GHz and 32 GB of RAM.

It is noted that, for a similar number of regression samples, the processing time of the RPC is much higher compared to the standard PCE, especially when the number of random parameters d is large. This is offset, however, by the much better accuracy achieved. Indeed, even by increasing the order of the single PCE, the accuracy remains well below the one obtained with the RPC model, while the processing times becomes larger because of the exorbitant requirement in terms of regression samples. Hence, the superior accuracy motivates the use of the RPC model in place of the single PCE despite its lower computational efficiency.

IX. Conclusions

This paper presented a novel RPC paradigm for modeling the stochastic responses of linear electrical networks. The new approach uses a ratio of PCEs with tensor degree truncation, rather than the conventional single PCE with total degree truncation. The model coefficients are computed with an iterative re-weighted linear least-square regression, whose samples are determined based on the distribution of the uncertain parameters. The proposed model is motivated by the precise form of the transfer function of linear lumped networks and, by extension, it is suitable for distributed systems as well. As a notable result, a first-order RPC model was shown to be exact for lumped networks. Several application test cases, including both lumped and distributed networks, were used for validation, demonstrating that the novel RPC model provides far superior accuracy w.r.t. the conventional single PCE. As a drawback, the calculation of the RPC model coefficients requires a larger processing time compared to the standard single PCE.

References

[1] J. Bai, G. Zhang, D. Wang, A. P. Duffy and L. Wang, "Performance comparison of the SGM and the SCM in EMC Simulation," *IEEE Trans. Electromagn. Compat.*, vol. 58, no. 6, pp. 1739–1746, Dec. 2016.

[2] P. Manfredi, D. Vande Ginste, I. S. Stievano, D. De Zutter, and F. G. Canavero, "Stochastic transmission line analysis via polynomial chaos methods: an overview," *IEEE Electromagn. Compat. Mag.*, vol. 6, no. 3, pp. 77–84, 2017.

[3] A. Kaintura, T. Dhaene, and D. Spina, "Review of polynomial chaos-based methods for uncertainty quantification in modern integrated circuits," Electronics, vol. 7, no. 3, p. 30:1–21, Feb. 2018.

[4] K. Strunz and Q. Su, "Stochastic formulation of SPICE-type electronic circuit simulation using polynomial chaos," *ACM Trans. Model. Comput. Simul.*, vol. 18, no. 4, pp. 15:1–15:23, Sep. 2008.

[5] M. R. Rufuie, E. Gad, M. Nakhla, and R. Achar, "Generalized Hermite polynomial chaos for variability analysis of macromodels embedded in nonlinear circuits," *IEEE Trans. Compon. Packag. Manuf. Technol.*, vol. 4, no. 4, pp. 673–684, Apr. 2014.

[6] P. Manfredi, D. Vande Ginste, D. De Zutter, and F. G. Canavero, "Stochastic modeling of nonlinear circuits via SPICE-compatible spectral equivalents," *IEEE Trans. Circuits Syst. I, Reg. Papers*, vol. 61, no. 7, pp. 2057–2065, Jul. 2014.

TABLE II
ACCURACY AND PROCESSING TIMES OF THE STANDARD PCE AND PROPOSED RPC FOR THE CONSIDERED TEST CASES.

Test case	d	PCE					RPC				
		p	K	max RMS error	max error	CPU time	p	K	max RMS error	max error	CPU time
Chebyshev filter	7	4	660	2.186×10^{-1}	1.442×10^{-0}	66.5 s	1	510	4.373×10^{-5}	8.731×10^{-4}	780.3 s
		6	3432	7.221×10^{-1}	4.424×10^{-0}	319.9 s					
		6	13728	2.555×10^{-2}	2.066×10^{-1}	1322.2 s					
Network with coupled microstrips	4	3	70	1.909×10^{-4}	9.803×10^{-4}	13.4 s	1	62	4.686×10^{-9}	1.606×10^{-8}	18.0 s
Network with coupled microstrips	2	6	224	5.298×10^{-2}	1.556×10^{-1}	81.3 s	3	248	5.233×10^{-4}	4.699×10^{-3}	138.8 s
		8	360	1.799×10^{-1}	4.855×10^{-1}	134.9 s					
		8	1440	9.243×10^{-3}	2.420×10^{-2}	537.9 s					
High-speed link	3	6	672	6.059×10^{-3}	2.683×10^{-2}	270.5 s	3	1016	2.403×10^{-4}	2.603×10^{-3}	983.4 s

[7] J. S. Ochoa and A. C. Cangellaris, "Random-space dimensionality reduction for expedient yield estimation of passive microwave structures," *IEEE Trans. Microw. Theory Tech.*, vol. 61, no. 12, pp. 4313–4321, Dec. 2013.

[8] P. Manfredi, D. Vande Ginste, D. De Zutter, and F. G. Canavero, "Generalized decoupled polynomial chaos for nonlinear circuits with many random parameters," *IEEE Microw. Wireless Compon. Lett.*, vol. 25, no. 8, pp. 505–507, Aug. 2015.

[9] M. Ahadi and S. Roy, "Sparse linear regression (SPLINER) approach for efficient multidimensional uncertainty quantification of high-speed circuits," *IEEE Trans. Comput.-Aided Des. Integr. Circuits Syst.*, vol. 35, no. 10, pp. 1640–1652, Oct. 2016.

[10] D. Spina, F. Ferranti, T. Dhaene, L. Knockaert, and G. Antonini, "Polynomial chaos-based macromodeling of multiport systems using an input-output approach," *Int. J. Numer. Model.*, vol. 28, no. 5, pp. 562–581, 2015.

[11] A. K. Prasad and S. Roy, "Accurate reduced dimensional polynomial chaos for efficient uncertainty quantification of microwave/RF networks," *IEEE Trans. Microw. Theory Tech.*, vol. 65, no. 10, pp. 3697–3708, Oct. 2017.

[12] M. Larbi, I. S. Stievano, F. G. Canavero, and P. Besnier, "Variability impact of many design parameters: the case of a realistic electronic link," *IEEE Trans. Electromagn. Compat.*, vol. 60, no. 1, pp. 34–41, Feb. 2018.

[13] Z. Zhang, X. Yang, I. V. Oseledets, G. E. Karniadakis, and L. Daniel, "Enabling high-dimensional hierarchical uncertainty quantification by ANOVA and tensor-train decomposition," *IEEE Trans. Comput.-Aided Des. Integr. Circuits Syst.*, vol. 34, no. 1, pp. 63–76, Jan. 2015.

[14] Z. Zhang, T.-W. Weng, and L. Daniel, "Big-data tensor recovery for high-dimensional uncertainty quantification of process variations," *IEEE Trans. Compon. Packag. Manuf. Technol.*, vol. 7, no. 5, pp. 687–697, May 2017.

[15] P. Benner, A. Cohen, M. Ohlberger, and K. Willcox. *Model Reduction and Approximation: Theory and Algorithms*. SIAM Publications, Philadelphia, PA, 2017.

[16] T. Chantrasmi, A. Doostan, and G. Iaccarino, "Padé-Legendre approximants for uncertainty analysis with discontinuous response surfaces," *J. Computational Physics*, vol. 228, no. 19, pp. 7159–7180, Oct. 2009

[17] E. Jacquelin, O. Dessombz, J.-J. Sinou, A. Adhikari, and M. I. Friswell, "Polynomial chaos-based Padé expansion in structural dynamics," *Int. J. Numerical Methods Eng.*, vol. 111. no. 12, pp. 1170-1191, Sep. 2017.

[18] M. Rossi, S. Agneessens, H. Rogier, D. Vande Ginste, "Stochastic analysis of the impact of substrate compression on the performance of textile antennas," *IEEE Trans. Antennas Propag.*, vol. 64, no. 6, pp. 2507–2512, Jun. 2016.

[19] D. Xiu and G. E. Karniadakis, "The Wiener-Askey polynomial chaos for stochastic differential equations," *SIAM J. Sci. Computation*, vol. 24, no. 2, pp. 619-622, 2002.

[20] C. Cui and Z. Zhang, "Stochastic collocation with non-Gaussian correlated process variations: theory, algorithms and applications," *IEEE Trans. Compon. Packag. Manuf. Technol.* (early access).

[21] J. Vlach and K. Singhal, *Computer Methods for Circuit Analysis and Design*, New York, NY, USA: Wiley, 1983.

[22] M.-D. Tong and W.-K. Chen, "On linear multivariable and multiloop feedback networks," *Trans. Circuits Syst.*, vol. 38, no. 8, pp. 869–874, Aug. 1991.

[23] C. K. Sanathanan and J. Koerner, "Transfer function synthesis as a ratio of two complex polynomials," *IEEE Trans. Autom. Control*, vol. 8, no. 1, pp. 56–58, Jan. 1963.

[24] P. Triverio, S. Grivet-Talocia, and M. S. Nakhla, "A parameterized macromodeling strategy with uniform stability test," *IEEE Trans. Adv. Packag.*, vol. 32, no. 1, pp. 205-215, Feb. 2009.

[25] S. Grivet-Talocia and B. Gustavsen, *Passive Macromodeling: Theory and Applications*, Hoboken, NJ, USA: Wiley, 2015.

PLACE PHOTO HERE

Paolo Manfredi (S'10–M'14–SM'18) received the M.Sc. degree in electronic engineering from the Politecnico di Torino, Torino, Italy, in 2009, and the Ph.D. degree in information and communication technology from the Scuola Interpolitecnica di Dottorato, Politecnico di Torino, in 2013.

From 2013 to 2014, he was a Postdoctoral Researcher with the EMC Group, Politecnico di Torino. From 2014 to 2017, he was a Postdoctoral Research Fellow of the Research Foundation–Flanders (FWO) with the Electromagnetics Group, Department of Information Technology, Ghent University, Ghent, Belgium. He is currently an Assistant Professor with the EMC Group, Department of Electronics and Telecommunications, Politecnico di Torino. His research interests comprise the several aspects of circuit and interconnect modeling and simulation, including statistical and worst-case analysis, signal integrity, and electromagnetic compatibility.

Prof. Manfredi was a recipient of an Outstanding Young Scientist Award at the 2018 Joint IEEE International Symposium on Electromagnetic Compatibility & Asia-Pacific Symposium on Electromagnetic Compatibility, the Best Paper Award at the 2016 IEEE Electrical Design of Advanced Packaging and Systems Symposium, the Best Oral Paper Award and the Best Student Paper Award at the 22nd and 19th IEEE Conference on Electrical Performance of Electronic Packaging and Systems, respectively, a Young Scientist Award at the XXX International Union of Radio Science General Assembly and Scientific Symposium, and an Honorable Mention at the 2011 IEEE Microwave Theory and Techniques Society International Microwave Symposium.

PLACE
PHOTO
HERE

Stefano Grivet-Talocia (M'98–SM'07–F'18) received the Laurea and Ph.D. degrees in electronic engineering from the Politecnico di Torino, Turin, Italy.

From 1994 to 1996, he was with the NASA/Goddard Space Flight Center, Greenbelt, MD, USA. He is currently a Full Professor of electrical engineering with the Politecnico di Torino. He co-founded the academic spinoff company IdemWorks in 2007, serving as the President until its acquisition by CST in 2016. He has authored over 150 journal and conference papers. His current research interests include passive macromodeling of lumped and distributed interconnect structures, model-order reduction, modeling and simulation of fields, circuits, and their interaction, wavelets, time-frequency transforms, and their applications.

Dr. Grivet-Talocia was a co-recipient of the 2007 Best Paper Award of the IEEE TRANSACTIONS ON ADVANCED PACKAGING. He received the IBM Shared University Research Award in 2007, 2008, and 2009. He was an Associate Editor of the IEEE TRANSACTIONS ON ELECTROMAGNETIC COMPATIBILITY from 1999 to 2001 and He is currently serving as Associate Editor for the IEEE TRANSACTIONS ON COMPONENTS, PACKAGING AND MANUFACTURING TECHNOLOGY. He was the General Chair of the 20th and 21st IEEE Workshops on Signal and Power Integrity (SPI2016 and SPI2017).